JSS Focus Issue on Visible and Infrared Phosphor Research and Applications

Preparation of a $Sr_{2-x}Eu_xSi_5N_8$ Phosphor Using an Ion Transporter

Tae Gil Lim,[a] Hongil Jo,[b] Yong Nam Ahn,[a] Kang Min Ok,[b] and Jae Soo Yoo[a,z]

[a]*School of Chemical Engineering and Materials Science, Chung-Ang University, Dongjak-gu, Seoul 06974, Korea*
[b]*Department of Chemistry, Chung-Ang University, Dongjak-gu, Seoul 06974, Korea*

We synthesized a single-phase $Sr_{2-x}Eu_xSi_5N_8$ phosphor using an ion transporter, $Sr_{3-x}Eu_x(PO_4)_2$, under atmospheric condition. This is a simple yet efficient synthetic route to the $Sr_{2-x}Eu_xSi_5N_8$phosphor. The quantum efficiency of the phosphor is 90.7%, and the absorption ratio of the excitation wavelength at 450 nm is 88.3%, even though the inexpensive and commercially available raw materials are used without any pretreatment and are easy to handle in a normal atmosphere including oxygen and moisture. We believe that this approach can be used to prepare other nitride-based phosphors, whose synthesis is currently challenging.

Manuscript submitted June 1, 2017; revised manuscript received July 12, 2017. Published July 27, 2017. *This paper is part of the JSS Focus Issue on Visible and Infrared Phosphor Research and Applications.*

White light-emitting diodes (WLEDs) were first developed by Nichia, and these are fabricated by coating $Y_3Al_5O_{12}:Ce^{3+}$ ($YAG:Ce^{3+}$), a yellow emitting phosphor which conducted studies to enhance luminescence properties,[1] onto a blue-emitting InGaN chip. WLEDS of this type are characterized by a high correlated color temperature (CCT) of 4000–8000 K and a low color rendering index (CRI) with an especially low R9 value. These characteristics limit the applications of WLEDs to general lighting as well as LCD backlighting. The addition of red phosphors to packaged WLEDs has been suggested as a solution to this problem.[2] Such phosphors include $CaS:Eu^{2+}$, $M_2Si_5N_8:Eu^{2+}$ (M = Ba, Sr, and Ca),[3] $Sr_2Si_3O_2N_4:Eu^{2+}$,[4] $CaAlSiN_3:Eu^{2+}$,[5] and $K_2SiF_6:Mn^{4+}$.[6] In addition, various other (oxy)nitride phosphors as $Ca_{1.5}Ba_{0.5}Si_5N_6O_3:Eu^{2+}$,[7,8] $Gd_3Al_{3+x}Si_{3-x}O_{12+x}N_{2-x}:Ce^{3+}$,[9] $La_3Si_6N_{11}:Ce^{3+}$,[10] $La_{4-x}Ca_xSi_{12}O_{3+x}N_{18-x}:Eu^{2+}$[11] for WLEDs have been studied.

One of the first commercialized red phosphors was the $Sr_{2-x}Eu_xSi_5N_8$ nitride phosphor, which was reported in 2005.[12] The crystal structure of $M_2Si_5N_8$ (M = Ca, Sr, and Ba) was investigated in 1995.[13] Nitride phosphors such as $Sr_{2-x}Eu_xSi_5N_8$have outstanding thermochemical stability and excellent photoluminescence properties, such as high emission intensity, high conversion efficiency, and very low thermal quenching. These outstanding properties result from the characteristics of Si_3N_4, which is a stable, covalently bonded material.[14] Because of their stability, it is difficult to synthesize nitride phosphors when silicon nitride is the main component of the phosphor structure, and high temperatures and pressures are required to ensure complete reaction. Intense attempts have been made to synthesize single-phase nitride phosphors. In some cases, unstable starting materials, such as metal nitrides that can easily react with moisture and oxygen, are needed. To synthesize the $Sr_{2-x}Eu_xSi_5N_8$phosphor, Sr^{2+} and Eu^{2+} ions must be substituted into the silicon nitride network, a three-dimensional network composed of corner-sharing SiN_4 tetrahedra. In addition, the nitride phosphor contains no oxygen.[15]

An example of the solid-state reaction method, the most common technique, is shown below.[16]

$$(2-x)\,Sr_3N_2 + 3xEuN + 5Si_3N_4 \rightarrow 3Sr_{2-x}Eu_xSi_5N_8 + 0.5xN_2 \quad [1]$$

This method is suitable for obtaining high-purity nitride phosphors. However, this synthetic method requires a very carefully controlled reaction environment. For example, the complete isolation of the reaction mixture from the atmosphere is required. In addition, the raw materials, such as Sr_3N_2, EuN, and α-Si_3N_4, are sensitive to oxygen and moisture. Thus, these commercially available materials must be handled carefully in a purified-nitrogen-filled glove box. The gas-reduction nitridation (GRN) method, which excludes oxygen, is shown in Eq. 2.[13]

$$(2-x)\,Sr + xEu + 5Si(NH)_2 \rightarrow Sr_{2-x}Eu_xSi_5N_8 + N_2 + 5H_2 \quad [2]$$

The starting materials $Si(NH)_2$ and EuN are sensitive to oxygen and moisture and require the use of a glove box. In contrast, some studies have shown that nitride phosphors can be synthesized from starting materials that are not sensitive to moisture and oxygen. The carbothermal reduction nitridation (CRN) method is shown in Eq. 3.[17]

$$(2-x)\,SrCO_3 + (5/3)\,Si_3N_4 + (x/2)\,Eu_2O_3 + 2C + N_2 \rightarrow Sr_{2-x}Eu_xSi_5N_8 + 3CO\uparrow \quad [3]$$

The CRN method has been used to prepare the $Sr_{2-x}Eu_xSi_5N_8$ phosphor by heating a mixture of powdered Si_3N_4, $SrCO_3$, Eu_2O_3, and C at 1500°C. The starting materials are inexpensive and insensitive to moisture and oxygen. However, after reaction, unreacted carbon remains, and this results in significantly lower luminescence of the phosphors. To remove the residual carbon, heating the sample in an oxygen-containing atmosphere is necessary. However, repeated heat-treatment results in significantly reduced luminescence properties. The gas pressure sintering (GPS) method, which is the most popular commercial method is shown in Eq. 4.[15]

$$2Si_3N_4 + (4-2x)\,SrCO_3 + (x/2)\,Eu_2O_3 \rightarrow Sr_{2-x}Eu_xSi_5N_8 + Sr_{2-x}Eu_xSiO_4 + 4CO_2\uparrow \quad [4]$$

In this method, the powder mixture is fired at 1600°C for 2 h in nitrogen at 0.5 MPa using a gas-pressure sintering furnace with a graphite heater. The synthesis method using high pressure is advantageous in that carbon powder is not used. However, it forms an impurity phase, $Sr_{2-x}Eu_xSiO_4$. Overall, the four previous synthesis methods tell us that two conditions are required for the synthesis of nitride phosphors. First, the starting materials should be stable under atmospheric conditions, including stability to oxygen and moisture. Secondly, Sr and Eu, which will be combined with the SiN_4 network, must be in a metallic or metal ion state during the high-temperature reaction. Consequently, we investigated how the careful selection of the starting materials can lead to the formation of a stable nitride host crystal lattice.

In this study, for the synthesis of highly pure Eu^{2+}-doped strontium silica nitride for use as a phosphor, the starting materials were investigated. Furthermore, the synthetic route of $Sr_{2-x}Eu_xSi_5N_8$ was also investigated by examining the reaction conditions, such as temperature and flow rate. We believe that this study will help to develop efficient and complete reaction routes for nitride-based phosphors.

[z]E-mail: jsyoo@cau.ac.kr

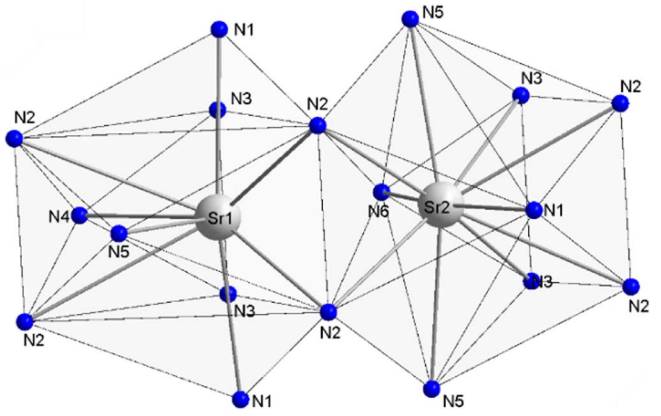

Figure 1. The part of structure of $Sr_2Si_5N_8$, which is appearance of Sr combined with coordinated nitrogen in SiN_4 networks.

Experimental

The silicon source used in these all experiments is silicon nitride, α-Si_3N_4(99.99%). Experiments using various strontium sources were conducted to set up experimental control groups and identify new synthesis routes for $Sr_{2-x}Eu_xSi_5N_8$. The strontium sources used in the experiments are $SrCO_3$ (99.99%), $Sr_3(PO_4)_2$ (99.99%), and $Sr_{3-x}Eu_x(PO_4)_2$. In the case of $SrCO_3$, a typical CRN method was used with a mixture of α-Si_3N_4(99.99%), Eu_2O_3(99.99%), and a small amount of carbon powder. Carbon powder was only used in experiments using the CRN method. In contrast, in the experiments using $Sr_{3-x}Eu_x(PO_4)_2$, α-Si_3N_4, and Eu_2O_3 were used with an excess of α-Si_3N_4. For $Sr_{3-x}Eu_x(PO_4)_2$, a stoichiometric mixture of $SrCO_3$, Eu_2O_3, and $NH_4H_2PO_4$(99.99%) was fired in an alumina crucible at 1200°C for 4 h under an N_2/H_2 atmosphere. The raw materials according to the specific composition were mixed in isopropyl alcohol (IPA) using silicon nitride balls for 24 h. Then, the ball-milled powder mixtures were loosely packed into carbon crucibles. No flux was added to the mixtures. Each prepared mixture was calcined at 1500°C for 7 h in a N_2/H_2 (90:10) atmosphere to obtain $Sr_{2-x}Eu_xSi_5N_8$. The value of x, indicating the europium concentration, was fixed at 0.04. Then, experiments were conducted for each experiment using $Sr_{3-x}Eu_x(PO_4)_2$ as the starting material. The synthesis temperature was varied between 1400 and 1600°C in intervals of 50°C. The maximum temperature holding time for all experiments was fixed at 7 h. Experiments were also performed to investigate the effect of the flow rate of hydrogen gas. When hydrogen was omitted from the gas flow, the experiments were conducted with nitrogen gas alone. The powders were mixed stoichiometrically and ball milled in IPA. The prepared mixture was placed in a carbon crucible and calcined at 1500°C for 7 h in an N_2/H_2(90:10) atmosphere, yielding $Sr_{2-x}Eu_xSi_5N_8$ ($x = 0.04$). All processes were carried out under normal atmospheric conditions in the presence of moisture and oxygen.

The obtained samples were washed in warm water to remove any residual materials. The synthesized phosphors were characterized by powder X-ray diffraction (XRD, Bruker, New D8-Advance-AXS, 40 kV and 40 mA) using Cu K_α radiation to identify the phase and crystal structure. The photoluminescence emission (PL) and excitation (PLE) spectra were recorded at room temperature using a photomultiplier tube and xenon lamp (PSI, Korea). The absorption ratio and internal quantum efficiency of the phosphor were obtained from the $BaSO_4$ coated integrating sphere with a photomultiplier tube and xenon lamp (PSI, Korea).

Results and Discussion

The Si_3N_4 component, the main structural component in $Sr_2Si_5N_8$, has a three-dimensional network structure composed of corner-sharing SiN_4 tetrahedra. It has high chemical and thermal stability and excellent mechanical properties because of the strong chemical bonds. These characteristics are connected to the high thermal stability of the nitride phosphor. However, its chemical stability makes the synthesis of Si_3N_4 difficult.[13] Figure 1 shows the structure of $Sr_2Si_5N_8$, which is reprinted from the literature.[18] The two Sr ions are coordinated by nitrogen atoms. In the Eu^{2+}-doped $Sr_2Si_5N_8$ phosphor, europium occupies the strontium sites. Because the ionic radius of the Eu^{2+} ion is similar to that of the Sr^{2+} ion, one can reasonably assume that Eu^{2+} is statistically distributed over the two available Sr sites.[13]

From an engineering point of view, the first step in synthesizing a pure nitride phase is to suppress the possibility of impurity formation through the phase diagram. This may be important in selecting starting materials. Studies utilizing various sources of strontium for the synthesis of pure nitride phosphors have been carried out to support the importance of the starting materials mentioned above. Figure 2 shows the Sr-Si-(O)-N phase diagram, which has been reported previously and confirmed through both calculations and experiments using the CRN method.[19] The formation of impurity phases and metastable phases, such as Sr_2SiO_4[15] and $SrSi_2O_2N_2$,[20] respectively, has also been confirmed previously. Thus, it is difficult to obtain a pure phase of $Sr_2Si_5N_8$ using an oxide as a starting material. In addition, the

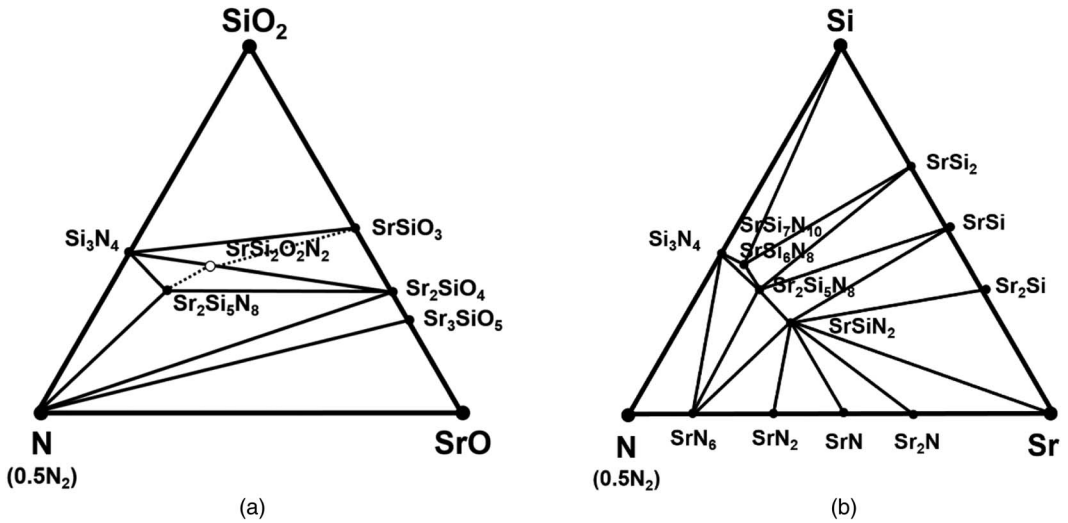

Figure 2. a. Experimental phase diagram of SrO-SiO_2-N system determined using the CRN method. b. Simulated phase diagram of Sr-Si-N system in which oxygen is excluded.

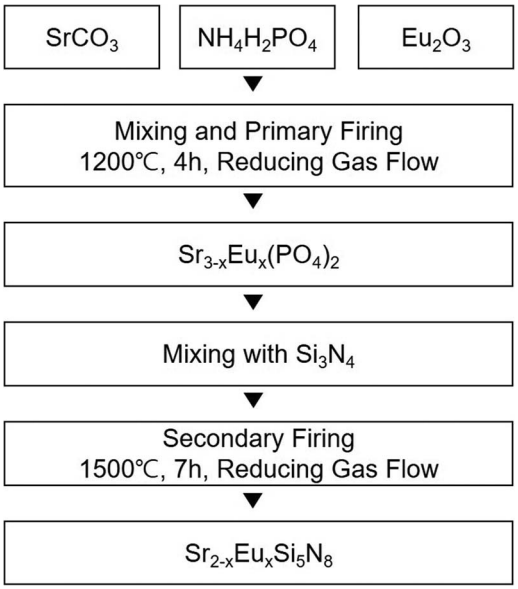

Figure 3. Process diagram for the synthesis of a nitride phosphor using $Sr_{3-x}Eu_x(PO_4)_2$.

$Sr_2Si_5N_8$, $SrSiN_2$,[21] $SrSi_6N_8$[22] and $SrSi_7N_{10}$[23] phases have been reported to be formed commonly. As mentioned, high synthetic temperatures are required to synthesize the $Sr_2Si_5N_8$ crystal phase, and multiple phases are often formed. To prevent the formation of undesirable phases such as $SrSiN_2$ and $SrSi_6N_8$, heating at relatively low temperatures is required. High purity nitride phosphors can be synthesized by the combination of silicon nitride and strontium nitride, as shown in Fig. 2, consistent with previous studies using sensitive materials, such as strontium nitride, to form high purity phases of $Sr_2Si_5N_8$. As shown in the phase diagram, $Sr_2Si_5N_8$ is in close proximity and connected by a straight line to silicon nitride and strontium metal. However, the use of pure metals as starting materials is limiting because the metals are easily oxidized by moisture and oxygen in the atmosphere. In addition, metals or metal nitrides are difficult to handle, resulting in prohibitive costs.

In this study, the intermediate reactants are used for efficient reaction. The basic idea is that oxygen should not participate in the reaction during synthesis at high temperatures. The reactions for the synthesis of a pure $Sr_{2-x}Eu_xSi_5N_8$ phase are shown in Eq. 5, 6 and 7.

$$(3-x)\,SrCO_3 + 2NH_4H_2PO_4 + (x/2)\,Eu_2O_3 \rightarrow 2Sr_{3-x}Eu_x(PO_4)_2 \quad [5]$$

$$2Sr_{3-x}Eu_x(PO_4)_2 + 6H_2 \rightarrow 2Sr^{2+}{}_{3-x}Eu^{2+}{}_x + 4H_3PO_4 \uparrow \quad [6]$$

$$2Sr^{2+}{}_{3-x}Eu^{2+}{}_x + 5Si_3N_4 + 2N_2 \rightarrow 3Sr_{2-x}Eu_xSi_5N_8 \quad [7]$$

The intermediate, $Sr_{3-x}Eu_x(PO_4)_2$, was used to obtain high purity $Sr_{2-x}Eu_xSi_5N_8$. It has a strong resistance to oxygen and moisture and contains oxygen. However, the oxygen atoms are removed from the phosphor during its formation. The reason for choosing Eu^{2+}-doped strontium phosphate is the difference in bond dissociation energies between Sr, P, O, and Eu. The oxygen atoms are removed during the reaction by forming phosphoric acid. The bond dissociation energy between Sr and O is 454 kJ/mol. The bond dissociation energy between P and O is 596.6 kJ/mol.[24] Consequently, less energy is needed to dissociate the Sr-O bonds than the P-O bonds. Based on the bond dissociation energies, strontium phosphate will decompose into Sr^{2+} and $PO_4{}^{3-}$, and, when certain conditions are met, SrO will not be formed. We have confirmed this experimentally. In our experiments, we confirmed that impurities such as Sr_2SiO_4 and $SrSi_2O_2N_2$ were formed when insufficient heating was used, as shown by the temperature-dependent experiments. The preparation of a pure $Sr_{2-x}Eu_xSi_5N_8$ phase results from the decomposition of the ion transporter, $Sr_{3-x}Eu_x(PO_4)_2$, at elevated temperatures. The process of synthesizing a nitride phosphor using the ion transport material is shown in Fig. 3.

The final products were obtained under the previously given conditions at a gas flow rate of 500 mL/min and a temperature of 1500°C. A maximum temperature holding time of 6 h was used. Figures 4a and 4b show the XRD patterns and PL spectra of the samples obtained from three starting mixtures, $SrO + C + Eu_2O_3$, $Sr_3(PO_4)_2 + Eu_2O_3$, and $Sr_{3-x}Eu_x(PO_4)_2$. The XRD patterns of these three samples were indexed and found to comprise mostly $Sr_2Si_5N_8$ (PDF 01-085-0101). There are no significant differences in the XRD profiles. However, the PL spectra in Fig. 4b show large differences in the emission intensities for samples produced from different starting materials. The phosphor prepared using $Sr_{3-x}Eu_x(PO_4)_2$ had the highest luminescence characteristics. On using undoped $Sr_3(PO_4)_2$ without carbon powder, Eu_2O_3 was not reduced to Eu^{2+}.

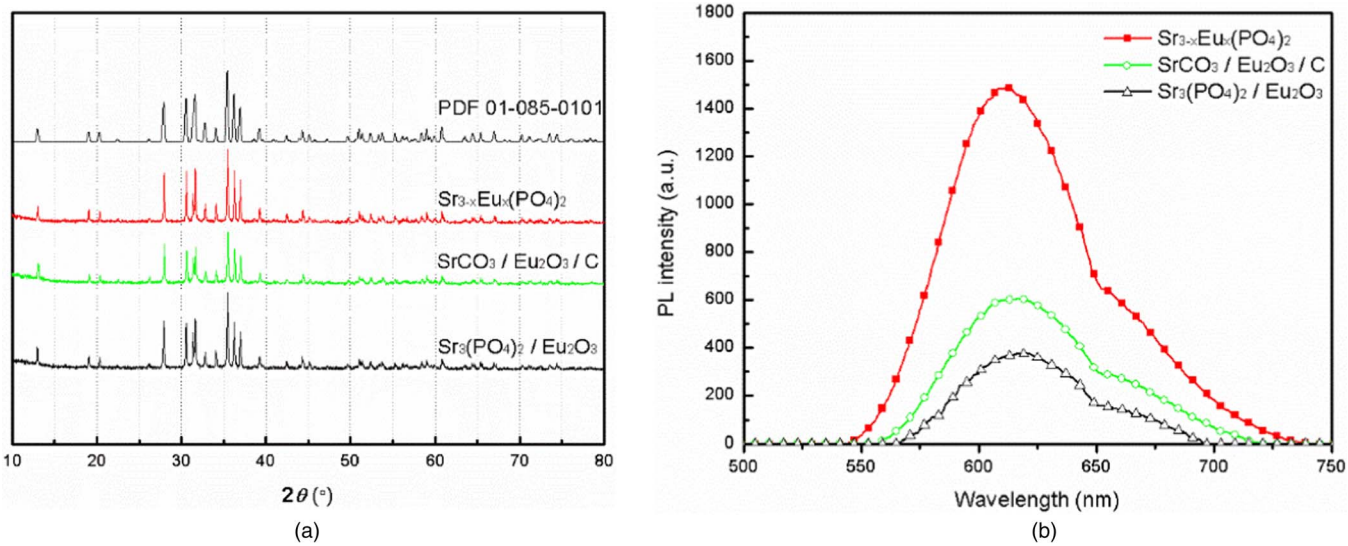

Figure 4. a. Powder X-ray diffraction (XRD) patterns of the samples prepared by using the CRN method, undoped $Sr_3(PO_4)_2$, and $Sr_{3-x}Eu_x(PO_4)_2$. b. PL spectra of the samples prepared by using CRN method, undoped $Sr_3(PO_4)_2$, and $Sr_{3-x}Eu_x(PO_4)_2$.

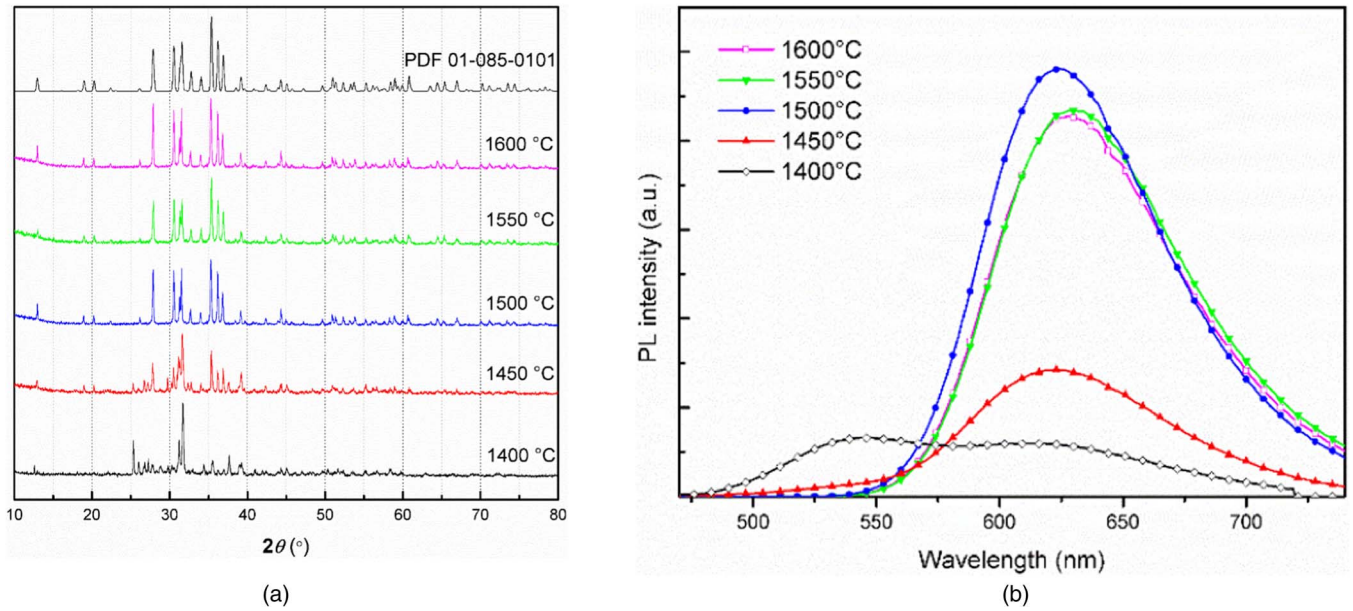

Figure 5. a. XRD data showing the effect of varying the temperature from 1400 to 1600°C. b. PL spectrum in the experiments at various temperatures from 1400 to 1600°C.

The internal quantum efficiency of the phosphor obtained using $Sr_{3-x}Eu_x(PO_4)_2$ was 90.7%, and absorption of 450 nm light was 88.3%. $BaSO_4$ powders with a reflectivity of ~100% in visible light were used as the standard to calculate the spectrum of the excitation source. The internal quantum efficiency and absorption ratio proceeded under the excitation at 450 nm. The internal quantum efficiency of the particle was calculated by the following equation:

$$\eta_i = \frac{\int \lambda \cdot P(\lambda)\, d\lambda}{\int \lambda \{E(\lambda) - R(\lambda)\}\, d\lambda} \quad [8]$$

where $E(\lambda)/h\nu$, $R(\lambda)/h\nu$ and $P(\lambda)/h\nu$ are the number of photons in the spectrum of excitation, reflectance, and emission of the phosphor, respectively.[25]

Subsequently, we optimized the reaction conditions to obtain a maximal luminescence intensity. The main reactions to obtain the $Sr_{2-x}Eu_xSi_5N_8$ phosphor is shown in Eqs. 6 and 7. To confirm the removal of phosphoric acid during synthesis, we carried out experiments at different synthesis temperatures. $Sr_3(PO_4)_2$ is stable, but it can be decomposed to supply Sr that can then be incorporated into the crystalline $Sr_2Si_5N_8$ network. For confirming reaction mechanism, two reaction routes are considered. The first one is:

$$Sr_3(PO_4)_2 + 3H_2 \rightarrow 3Sr + 2H_3PO_4 \quad (\Delta H = +1554.1\ kJ/mol) \quad [9]$$

The standard enthalpies of formation of $Sr_3(PO_4)_2$, H_2, Sr, and H_3PO_4 are −4122.9, 0, 0, and −1284.4 kJ/mol, respectively.[24] The reaction enthalpy of Eq. 7 is 1554.1 kJ/mol, so this is an endothermic reaction. At least 1554.1 kJ of heat must be absorbed for the reaction shown in Eq. 9 to proceed. As a result, the supply of hydrogen gas should result in the formation of H_3PO_4. The boiling point of H_3PO_4 is 175°C. As such, it is immediately evaporated at the reaction temperature. Calcium phosphate and barium phosphate decompose at 1112 and 1727°C, respectively. The melting point of the $Sr_3(PO_4)_2$ is estimated to range from 1112 to 1727°C and, thus, lies within the reaction temperature range. The excess H_2 gas flow requires the $(PO4)^{3-}$ ion transporter. The $Sr_3(PO_4)_2$ will be decomposed into Sr^{2+} and H_3PO_4, which are recombined with $(PO4)^{3-}$ at elevated temperatures and under the continuous flow of hydrogen gas. The second one is:

$$Sr_3(PO_4)_2 + 8H_2 \rightarrow 2PH_3 + 3SrO \quad (\Delta H = +928\ kJ/mol) \quad [10]$$

This route is thermodynamically easier reaction route than that of previous reaction Eq. 9. However, we could not observe any crystal phases of SrO, PH_3 and H_3PO_4 from the XRD data after final products. Also, it was confirmed that the reaction route took the Eq. 9 at our experimental require by comparing the weight difference before and after the experiment. The weight before the experiment was 4 g, and the weight after the experiment was about 3 g. The difference of about 1 g was consistent with the weight of H_3PO_4, which was supposed to have escaped during the reaction. This is equivalent to the loss of 4 moles of H_3PO_4 during the synthesis of 3 moles of $Sr_2Si_5N_8$. Considering these two experimental observations, we concluded that the decomposition process in our experimental regime would have proceeded in reaction route of the Eq. 9. Then, Sr ions combines with Si_3N_4 network to become final product.

Figure 5a shows the XRD data in the experiments at various temperature ranging from 1400 to 1600°C. The changes in the XRD profiles demonstrate the phase change. As shown in Fig. 5a, the $Sr_2Si_5N_8$ phase increased, while the Sr_2SiO_4 and $SrSi_2O_2N_2$ phases decreased as the experimental temperature increased from 1400 to 1500°C. Above 1500°C, only the $Sr_2Si_5N_8$ crystalline phase is observed, and no impurities are present. Figure 5b shows the PL spectra in the variable temperature experiments (1400 to 1600°C). The XRD data and PL spectra both show that the ratio of the $Sr_2Si_5N_8$ phase increases as the synthesis temperature increases. However, when the synthesis temperature exceeds 1500°C, the luminescence characteristics were reduced. Despite this, the $Sr_2Si_5N_8$ phase has been reported to be formed only at temperatures significantly greater than 1500°C.

Figures 6a and 6b show the effect of the flow rate of 5% H_2/N_2 gas on the XRD diffraction patterns and PL spectra. The phosphate reacted with H_2 gas, forming phosphoric acid that was removed at high flow rates. Figure 6 shows that phosphoric acid is not removed when N_2 gas is supplied alone. The remaining oxygen atoms of phosphoric acid and silicon nitride are combined to form the $SrSi_2O_2N_2$ phase.

Conclusions

In conclusion, we have reported a novel synthetic route to obtain red phosphors via the intermediate reaction of $Sr_{3-x}Eu_x(PO_4)_2$ and Si_3N_4 at 1500°C under atmospheric condition. In this experiment, a mixture of 10% H_2/90% N_2 was used as the reducing gas. It was found that the ion transporter, $Sr_{3-x}Eu_x(PO_4)_2$, was very effective to prepare the target phosphor material, and the reaction occurred at relatively low temperatures under atmospheric condition. Furthermore, the reaction

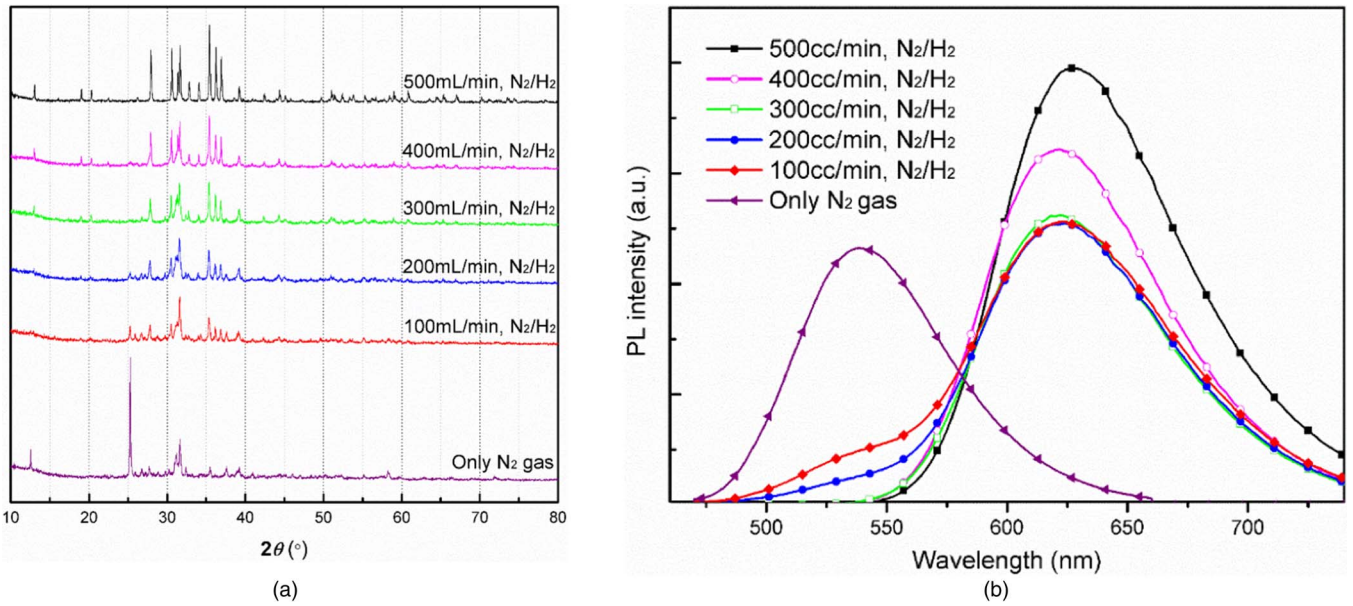

Figure 6. a. XRD data showing the effect of reducing the gas flow rate from 100 to 500 mL/min. b. PL spectrum showing the effect of varying the reducing gas flow rate from 100 to 500 mL/min.

proceeded even in the presence of oxygen. We investigated synthetic routes toward stable phosphor materials, such as Si_3N_4. This method of synthesis does not leave residual carbon and does not require high pressures. In addition, the starting materials are inexpensive, commercially available, and easy to handle in a normal atmosphere including oxygen and moisture. Thus, the method offers a simple, efficient, and high-yield route to $Sr_{2-x}Eu_xSi_5N_8$. We believe that this approach is also applicable to the synthesis of other nitride-based phosphors.

Acknowledgments

This work was supported by the Technology Innovation Program (or Industrial Strategic Technology Development Program (10053623, Development of Green-LED-Based Indoor Lighting Module with High CRI index above 95) funded by the Ministry of Trade, Industry & Energy (MI, Korea).

References

1. M. S. Jang, Y. H. Choi, S. Wu, T. G. Lim, and J. S. Yoo, *Journal of Information Display*, **17**(3), 117 (2016).
2. M. Yamada, T. Naitou, K. Izuno, H. Tamaki, Y. Murazaki, M. Kameshima, and T. Mukai, *Japanese Journal of Applied Physics Part 2-Letters & Express Letters*, **42**(1a-B), L20 (2003).
3. Y. Q. Li, J. E. J. van Steen, J. W. H. van Krevel, G. Botty, A. C. A. Delsing, F. J. DiSalvo, G. de With, and H. T. Hintzen, *Journal of Alloys and Compounds*, **417**(1–2), 273 (2006).
4. G. Anoop, K. P. Kim, D. W. Suh, I. H. Cho, and J. S. Yoo, *Electrochem. Solid State Lett.*, **14**(9), J58 (2011).
5. K. Uheda, N. Hirosaki, Y. Yamamoto, A. Naito, T. Nakajima, and H. Yamamoto, *Electrochem. Solid State Lett.*, **9**(4), H22 (2006).
6. H. Zhu, C. C. Lin, W. Luo, S. Shu, Z. Liu, Y. Liu, J. Kong, E. Ma, Y. Cao, R. S. Liu, and X. Chen, *Nat. Commun.*, **5**, 4312 (2014).
7. W. B. Park, H. Kim, H. Park, C. Yoon, and K. S. Sohn, *Inorg. Chem.*, **55**(5), 2534 (2016).
8. W. B. Park, S. P. Singh, C. Yoon, and K. -S. Sohn, *Journal of Materials Chemistry C*, **1**(9), 1832 (2013).
9. W. B. Park, S. P. Singh, M. Kim, and K. S. Sohn, *Inorg. Chem.*, **54**(4), 1829 (2015).
10. W. B. Park, T. H. Kwon, K. -S. Sohn, and J. A. Varela, *Journal of the American Ceramic Society*, **98**(2), 490 (2015).
11. W. B. Park, Y. Song, M. Pyo, and K. S. Sohn, *Opt. Lett.*, **38**(10), 1739 (2013).
12. R. Mueller-Mach, G. Mueller, M. R. Krames, H. A. Höppe, F. Stadler, W. Schnick, T. Juestel, and P. Schmidt, *physica status solidi (a)*, **202**(9), 1727 (2005).
13. T. Schlieper, W. Milius, and W. Schnick, *Zeitschrift fr anorganische und allgemeine Chemie*, **621**(8), 1380 (1995).
14. K. Van den Eeckhout, P. F. Smet, and D. Poelman, *Materials*, **4**(12), 980 (2011).
15. R. J. Xie, N. Hirosaki, T. Suehiro, F. F. Xu, and M. Mitomo, *Chemistry of Materials*, **18**(23), 5578 (2006).
16. Y. Q. Li, G. de With, and H. T. Hintzen, *Journal of Luminescence*, **116**(1–2), 107 (2006).
17. X. Q. Piao, T. Horikawa, H. Hanzawa, and K. Machida, *Applied Physics Letters*, **88**(16), 161908 (2006).
18. S. R. Romer, C. Braun, O. Oeckler, P. J. Schmidt, P. Kroll, and W. Schnick, *Chemistry*, **14**(26), 7892 (2008).
19. Y. Kim, J. Kim, and S. Kang, *J. Mater. Chem. C*, **1**(1), 69 (2013).
20. L. Chen, S. Xue, X. Chen, E. Zhao, J. Deng, X. Deng, S. Chen, Y. Liu, Y. Jiang, and H. Li, *RSC Adv.*, **4**(83), 44317 (2014).
21. L. Chen, R. H. Liu, W. D. Zhuang, Y. H. Liu, Y. S. Hu, X. L. Ma, and B. Hu, *Journal of Rare Earths*, **34**(1), 30 (2016).
22. S. -M. Wu, H. -E. Hung, C. -H. Hsieh, Y. -C. Lin, L. -C. Wang, Y. -T. Tsai, C. C. Lin, R. -S. Liu, and H. Hintzen, *Journal of the American Ceramic Society*, **98**(8), 2662 (2015).
23. G. Pilet, H. A. Höppe, W. Schnick, and S. Esmaeilzadeh, *Solid State Sciences*, **7**(4), 391 (2005).
24. J. Dean, *Lange's Handbook of Chemistry*, p. 625, McGRAW-HILL, INC.,(1999).
25. K. Ohkubo and T. Shigeta, *J. Illum. Eng. Inst. Japan*, **83**, 87 (1999).